Taylor & Francis
Taylor & Francis Group

Retrieval of marine water constituents from AVIRIS data in the Hudson/Raritan Estuary

S. BAGHERI*†, S. PETERS‡ and T. YU†

†Department of Civil and Environmental Engineering, New Jersey Institute of Technology, Newark, NJ 07102, USA
‡Vrije Universiteit, Amsterdam, The Netherlands

This paper reports on the validation of bio-optical models in estuarine and nearshore (case 2) waters of New Jersey–New York to retrieve accurate water leaving radiance spectra and chlorophyll concentration from the NASA Airborne Visible Infrared Imaging Spectrometer (AVIRIS) data complemented with *in situ* measurements. The study area—Hudson/Raritan Estuary—is a complex estuarine system where tidal and wind-driven currents are modified by freshwater discharges from the Hudson, Raritan, Hackensack, and Passaic rivers. Over the last century the estuarine water quality has degraded, in part due to eutrophication, which has disrupted the pre-existing natural balance, resulting in phytoplankton blooms of both increased frequency and intensity, increasing oxygen demand and leading to episodes of hypoxia. During 1999–2001 data acquisitions by NASA AVIRIS field measurements were obtained to establish hydrological optical properties of the Hudson/Raritan Estuary: (1) concurrent above- and below-surface spectral irradiance; (2) sampling for laboratory determination of inherent optical properties; and (3) concentrations of optically-important water quality parameters. We used a bio-optical model based on Gordon *et al.* to predict the sub-surface irradiance reflectance from optically important water constituents. Modelling of reflectance is a prerequisite for processing remote sensing data to desired thematic maps for input into the geographical information system (GIS) for use as a management tool in water quality assessment. A Radiative Transfer Code—MODTRAN-4—was applied to remove the effects of the atmosphere so as to infer the water leaving radiance from the AVIRS data. The results of this procedure were not satisfactory, therefore an alternative approach was tested to directly correct the AVIRIS image using modelled spectra based on measured optical characteristics. The atmospherically corrected AVIRIS ratio image was used to calculate a thematic map of water quality parameters (i.e. chlorophyll-a) concentration, which subsequently were integrated into a GIS for management of water quality purposes.

1. Introduction

Estuarine/nearshore waters (case 2) are very complex, being both spatially and temporally heterogeneous. This has created a persistent need for timely information to support a balanced approach to the use and protection of such waters, and

*Corresponding author. Tel: (973)-596-2470, Fax: (973)-596-9057, Email: bagheri@adm.njit.edu

numerous efforts are underway to improve the understanding of their physical, chemical, and biological characteristics. One approach uses remote sensing, offering unique advantages for the study of recurrent hydrological phenomena on regional and local scales. Overhead sensors record the colour of natural water as spectral reflectance, determined by the composition of the upwelling underwater light field. The greater the amount and specificity of colour information available, the better a remote hydrological application will generally perform. This is particularly true for estuarine applications, where independent variations of optically-important water quality parameters (WQP), bottom cover types, and water depths can all occur simultaneously. At the same time, all hydrological targets share general characteristics induced by the water medium itself. For example, there is a strong absorption of light with wavelengths shorter than those of blue light or with wavelengths longer than those of near-infrared light. Outside these limits, signals within or beneath any hydrological volume are attenuated so much, that the signals are negligible for practical remote detection.

Understanding the relationship between reflectance, absorption and back-scattering of water is essential for developing the analytical and multi-temporal algorithms necessary to use remote sensing as a management tool in the estuarine environment. To develop analytical algorithms for case 2 waters, an optical model needs to link the WQP to the inherent optical properties (IOP), linking these in turn to the sub-surface irradiance reflectance ($R(0-)$). *In situ* measurements of $R(0-)$ are used to validate model simulations of $R(0-)$. They are also used to calibrate and validate the atmospheric correction of observations from high platforms (aircrafts, satellites). Being able to remove atmospheric effects from the Airborne Visible Infrared Imaging Spectrometer (AVIRIS) observations of the study area (which provides AVIRIS observations of $R(0-)$), opens the way to apply the calibrated optical model inversely to the spectra in order to derive quantitative thematic maps of WQP. Thus $R(0-)$ is the key modelling parameter to translate remote observations of water leaving radiance into, for example, a thematic map of chlorophyll-a (CHL) concentration which, subsequently, can be used for input into a geographical information system (GIS) database of the study area to monitor and manage the estuarine water resources.

2. Physical characteristics of the study area

The study area was the Hudson/Raritan Estuary south of the Verrazano Narrows and bordered by western Long Island, Staten Island, and New Jersey (figure 1). The east–west extent of the Hudson/Raritan Estuary is about 20 km, and the average depth of the estuary is about 8 m). The Estuary constitutes an extremely complex system involving the interaction of tidal and wind-driven currents modified by the freshwater discharges from Hudson, Raritan, Hackensack, and Passaic rivers. Circulation in the Hudson/Raritan Estuary is the result of the combined effects of freshwater discharge, wind, and tide. The circulation is governed by two factors:

(1) the geometry of the estuary with open boundaries; and
(2) the surface wind stress, which is considered part of the surface boundary conditions (Oey *et al.* 1985).

Jeffries (1962) estimated the flushing time for the estuary to be 16–21 days (32–42 tidal cycles), which contributes to the accumulation of pollutants derived from municipal and industrial wastewater discharges, land runoff, and combined sewer
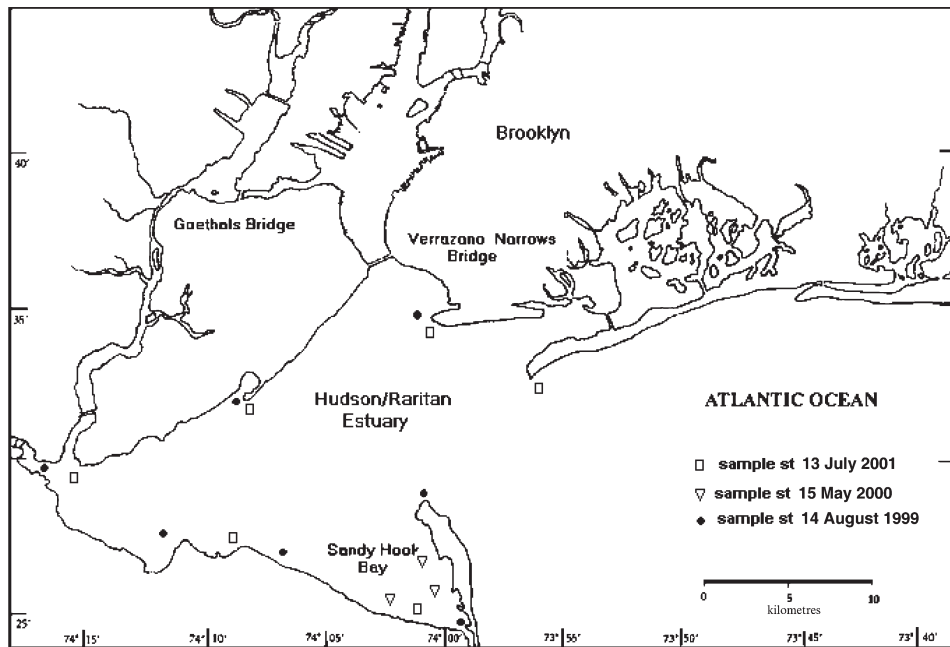
Figure 1. Map of the study area with the locations of the sample points.

outflows causing low dissolved oxygen. Also, the discharges of nitrogen and phosphorus to these waters stimulates algal growth causing eutrophication.

Over the last century the quality of the estuarine water has degraded, in part due to eutrophication. Eutrophication disrupts the pre-existing natural balance of the system, resulting in phytoplankton blooms of both increased frequency and intensity in response to the over-enrichment. Noxious phytoplankton blooms are among the potential negative impacts, as are shifts to less desirable species of phytoplankton, diminished aesthetics, and changes in phytoplankton cell size. Dense and accelerated phytoplankton blooms ultimately increase oxygen demand on the system leading to episodes of hypoxia. Table 1 lists the sampling stations, which were selected in diverse parts of the estuary to have maximum taxonomic variability in phytoplankton community; their IOP and WQP data obtained during the course of the project.

3. Materials and methods

3.1 In situ *measurements*

The research was based on data from the AVIRIS imaging spectrometer, two types of field spectroradiometers and water samplings. Based on these measurements a calibrated optical water quality model was constructed linking the water constituent concentrations to (i) the IOP, using the specific inherent optical properties (SIOP), and (ii) to the sub-surface (ir)radiance reflectance (Bagheri *et al*. 2000, 2001, 2002). Thus a simple optical water quality model was calibrated on measurements of optical water constituent concentrations and IOP and used to simulate sub-surface irradiance reflectance (or water leaving radiance). The following is a brief description of the research materials and methods used to (1) measure spectral

Table 1. Sample locations and water conditions as recorded onboard the research vessels.

Date	St	Location	Latitude (°)	Longitude (°)	SD (m)	TCHL $(mg\,m^{-3})$	TSM $(g\,m^{-3})$
14 August	1	Comptons/PewsCreek	40.45	74.08	1.3	15	6
1999	2	Keyport Harbor	40.47	74.19	0.8	32	26
	3	Traid Bridge	40.50	74.28	0.9	17	13
	4	Crookes Pt State Island	40.54	74.14	0.6	37	15
	5	Coney Island Pt	40.57	74.02	1.8	6	11
	6	Sandy Hook Tip	40.49	74.02	0.9	22	12
	7	Shrewsbury River	40.38	73.98	0.5	48	21
15 May	1	Buoy 2	40.42	74.01	1.25	31	8
2000	2	Atlantic Highlands	40.47	74.03	1.25	46	11
	3	Horseshoe Cove	40.59	74.03	1.37	22	7
13 July	1	Tip of Sandy Hook	40.55	73.93	1.3	38	23
2001	2	Ambrosa Channel	40.54	74.02	0.8	17	8
	3	Great Kills	40.52	74.13	0.9	36	23
	4	Raritan River	40.49	74.24	0.6	32	21
	5	Point Comfort	40.46	74.14	1.8	73	5
	6	Sandy Hook Bay	40.42	74.03	0.9	38	8

irradiance reflectance *in situ*, (2) measure the *in situ* concentration of optically active water constituents from water samples, and (3) establish the IOP of the estuary for retrieval of water quality concentrations from the AVIRIS data.

3.1.1 Spectral irradiance reflectance measurements. Table 1 shows the descriptions of the sample points where the spectral irradiance reflectance R(0-) above and below the water surface was measured during the course of the project (1999–2001). The reflectance measurements were obtained by simultaneously using two types of field spectroradiometers: (1) OL 754 (Optronic Laboratories), and (2) PR 650 (Photo Research).

Each spectroradiometer had a different design. The methods of dispersing the incoming light field, as well as the optical detectors registering the number of photons, were different for each spectroradiometer. The OL754 was designed for underwater measurements of upwelling and downwelling irradiances and was the primary instrument used for the seasonal field data collections during the term of the project. The PR650 was designed for radiance measurements in above-surface applications. Additional specifications for the field spectroradiometers that were used for the field measurements during the 14 August 1999 field campaign are given in Gons (1999) and Bagheri *et al*. (2000). Here the reference is given to the OL754 as the primary instrument used during the course of the project (1999–2001).

Upwelling ($E_u(\lambda)$) and downwelling ($E_d(\lambda)$) irradiances were measured by the submersible sphere assembly in both direct and reverse modes. This assembly was placed into the water at approximately 0.5 m below the surface. This depth was chosen because it was generally deeper than the maximum wave amplitude, which minimized the effects of waves. The time needed to complete a full scan was 3 mins at 10 nm interval covering the spectral range (300–850 nm). The sub-surface irradiance reflectance R(0-) in percentage was calculated as a ratio of $E_u(\lambda)$ to $E_d(\lambda)$ irradiance in units of $(W/(cm^{-2}\,nm))$ for the intercomparison process. At some stations, the influence of wave propagations was shown in the spectra acquired by the OL754. Generally, wave refraction problems caused by the modulation of light

and alternating focusing and defocusing cycles were produced by the motion and shape of the waves.

Comparisons of the reflectance spectra for all sampling stations showed that the results of the two spectroradiometers differed somehow; however, the range of values were quite consistent (i.e. 1–5% $R(0-)$ over the wavelength range of 480–700 nm) (figure 2).

3.1.2 Optical water quality concentration measurements. To estimate optical water quality concentrations coinciding with the spectral reflectance measurements, sub-surface water samples (0.2–0.5 m depth) were taken in 1-1 bottles and placed in a cooler with melting ice before transport to the laboratory for analysis. Standard procedures as described by Rijkeboer *et al.* (1998) were used to determine the concentrations of total chlorophyll-a (TCHL) defined as the sum of CHL and phaeopigments (as indication of concentration of phytoplankton) and total suspended matter (TSM). The pigment concentration was determined according
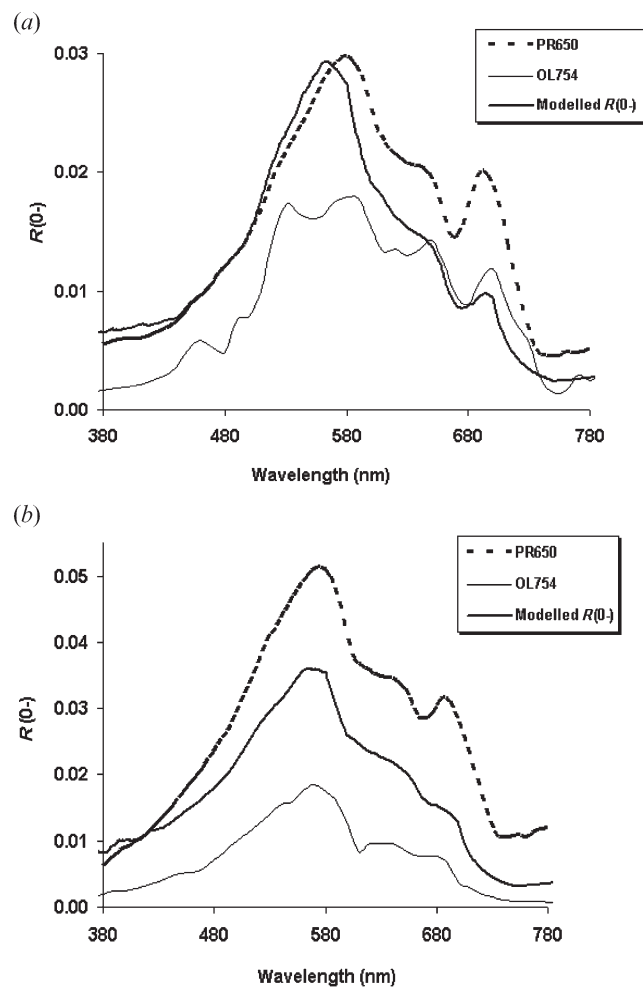

Figure 2.   Comparisons of modelled $R(0-)$ and measured (in water) $R(0-)$ using OL-754 and PR-650 spectroradiometers for (*a*) St3 (Traid Bridge) and (*b*) St4 (Crookes Point).

to the Dutch standard method Netherlands Standard Norms (NEN) 6520 (1981). This method is based on the extraction of CHL pigments from the phytoplankton using hot ethanol (80% at 75°C). The TCHL is then determined spectrophotometrically, using the extinction of the solvent at 665 nm and 750 nm. The phaeopigment concentration is determined similarly after acidification of the sample. All analyses were performed in duplicates. The TSM concentrations were determined according to the Dutch standard method NEN 6484 (1982). The samples were filtered over 0.45 μm Whatman GF/F filters with volumes ranging from 100 ml to 200 ml. The filters were dried at 80°C. Ignition loss was determined by ashing the filters with TSM at 550°C. The filters were flushed with 10 ml tap water to prevent overestimating the TSM concentration due to remaining salt left on the filter. Table 1 shows the concentration of WQP as sampled during 1999–2001, indicating that sampling did not coincide with any major phytoplankton bloom. Likewise, the TSM ranges were within the expected values for the time of year when the measurements taken.

Samples were also analysed for identification and enumeration of the phytoplankton species to demonstrate the variety and composition of phytoplankton populations for input into library spectra of the estuary, which is currently in progress (Bagheri *et al.* 1999). The most abundant organisms identified were the diatoms *Leptocylindrus minimus* and *Skeletonema costatum* in moderated counts (400 and 160 cells/ml, respectively). Also present in low counts were dinoflagellates *Gyrodinium* sp. (60 cells/ml) and *Katodinium colundatum* (80 cells/ml).

3.1.3 Inherent optical properties measurements. The two main IOP are the spectral absorption and scattering. Absorption is mainly caused by organic particles and dissolved organic while scattering is mainly caused by inorganic particles. The spectral absorption causes a reduction in $R(0\text{-})$, and the spectral scattering causes an increase in $R(0\text{-})$. Spectral beam attenuation (c) and spectral absorption (a) were obtained using Ocean Optics-2000. The Ocean Optics-2000 is a modular spectrophotometric/spectroradiometric system relying on optical fibres and fore-optics to enable it to carry out a variety of optical measurements. (Note: use of Ocean Optics-2000 for measuring IOP is experimental and has not been referenced in the published literature.) From these measurements, the spectral scattering (b) was deduced via subtraction of spectral absorption from the spectral beam attenuation ($b=c-a$). The samples were filtered through a 0.45 μm Whatman GF/C glassfibre filter. Then the coloured dissolved organic matter (CDOM) absorption was measured in a 10 cm cuvette against de-ionized (DI) water. The CDOM absorption spectra were normalized at 440 nm, and the absorption at 440 nm was taken as a measure of the concentration (Rijkeboer *et al.* 1998).

The seston (TSM) absorption spectra were measured using the filterpad method. After extraction of the ethanol-soluble pigments from the filter using approximately 5–10 ml hot (80°C) 80% ethanol, the absorption spectra of bleached seston were measured using the filterpad method. Phytoplankton absorption was calculated as the difference between seston absorption and bleached seston absorption. Scattering was calculated as the difference of the beam attenuation and the total absorption (seston + CDOM). TSM specific scattering and absorption were calculated by dividing the total scattering and total (seston) absorption by the simultaneous measurement of TSM concentrations. TCHL specific phytoplankton absorption was calculated by dividing the phytoplankton absorption with the TCHL concentration. These data as shown in table 1 and discussed below were used to

simulate sub-surface irradiance reflectance (or water leaving radiance) and to estimate the concentrations of various WQP.

3.2 *Calibration of Gordon's optical water quality model*

Several models for ocean, coastal and inland waters were investigated by Gordon *et al.* (1975), Morel and Prieur (1977), Whitlock *et al.* (1981), Kirk (1991) and Dekker and Donze (1994). A simple optical water quality model based on the work of Gordon *et al.* (1975) was calibrated for measurements of optical water constituent concentrations and IOP:

$$R(0-) = r(b_b/(a+b_b)) \tag{1}$$

where a is the total absorption coefficient; b_b the backscatter coefficient; and r a factor based on the geometry of incoming light and volume scattering in the water.

To establish values for r and b_b for a specific location, knowledge of the volume scattering function is required. Vos *et al.* (1998) demonstrated that a practical solution for measurement of the volume scattering function is to estimate r and b_b by matching modelled $R(0-)$ to measured $R(0-)$ values. According to Kirk (1991), the factor r for a large number of waterbodies measured varied between 0.34 and 0.39 depending on the solar zenith angle and atmospheric conditions. Dekker *et al.* (1997) reported that the r values ranged from 0.12 to 0.56 with an average of 0.29 for four inland water types in The Netherlands. These water types were: shallow eutrophic lakes, shallow mesotrophic lakes, deep lakes, and river and canals. In this study, the values for factor r varied between 0.30–0.38 and were based on the field data obtained in the estuary during the course of the project and calculations made by fitting measured $R(0-)$ spectra to measured IOP. The IOP a and b_b were assumed to be linear functions of the constituent concentrations. This allowed the SIOP to be introduced that link the concentrations of all optically active components to the sub-surface irradiance reflectance. The IOP per unit concentration, e.g. the specific inherent absorption by phytoplankton, $a*ph$, was the absorption caused by $1\,\mathrm{mg\,m}^{-3}$ CHL. Using Beer's law, the total absorption coefficient a can be written as sum of the absorption by phytoplankton, TSM, CDOM, and water. The concentrations of the constituents are given by CHL, TSM, and $CDOM_{440}$. It should be noted that specific absorption for CDOM could not be calculated because no concentrations of dissolved organic carbon (DOC) or particulate organic carbon (POC) were measured. Therefore, the CDOM absorption measured at 440 nm was taken as measure of concentration. The values for absorption coefficient (a_w) and the scattering coefficient (b_w) of pure water were taken from Bukata *et al.* (1995).

The backscattering (b_b) is used here which is based on the conversion of the scattering coefficient to the backscattering coefficient. The volume scattering function of Petzhold (Kirk 1994) is assumed to be valid, therefore b_b was obtained as $0.019b$. For pure water, this ratio is 0.5 but for seston measurements depends on the composition of the water (Morel and Prieur 1977).

$$a = a_w + a*_{TSM}\mathrm{TSM} + a*_{ph}\mathrm{CHL} + a*_{CDOM}\mathrm{CDOM}_{440} \tag{2}$$

$$b_b = 0.5 \bullet b_w + b_b*_{TSM}\mathrm{TSM} \tag{3}$$

where a_w is the absorption of pure water; $a*_{ph}$ the specific absorption of the phytoplankton; $a*_{TSM}$ the specific absorption of TSM; $a*_{CDOM}$ the specific

absorption of CDOM; b_w the scattering of pure water; b_b*_{TSM} the specific backscatter of TSM; 0.5 the backscatter to scatter ratio of pure water.

(Note: The asterisks denote that a and b_b are SIOP per unit concentration denoted by the subscript.)

The next step was to parametrize the bio-optical model by relating concentrations of CDOM, TSM and algal pigment concentrations to light absorption and scattering. Using the bio-optical model, $R(0-)$ spectra were simulated for the measured concentrations (using measured IOP). The subsequent comparison between simulated and measured $R(0-)$ provides a means to validate the bio-optical model and the accuracy of the field spectroradiometer measurements. Upon successful evaluation, the *in situ* measured $R(0-)$ spectra can also be used to validate atmospherically corrected remote sensing observations of reflectance spectra. The bio-optical model can further be used to simulate spectra at locations where some (general) knowledge exists of the concentrations of optically active water constituents (e.g. very dark and thus clear water locations on the image (figure 3)). This may lead to additional possibilities to calibrate the atmospheric correction of remote sensing observations. The inversion of the calibrated bio-optical model (using semi-analytical algorithms) can be used to characterize the estuarine waters in terms of CHL concentration, CDOM and TSM from the observed spectra.

3.3 Simulation modelling and retrieval techniques

A number of inverse modelling algorithms (Hoge and Lyon 1996, Hoogenboom *et al.* 1998, Hakvoort *et al.* 2000, Peters 2001) have been developed to retrieve the concentrations of optically active WQP. All these methods are based on inverting the Gordon's analytical model using matrix inversion techniques. The simplest form
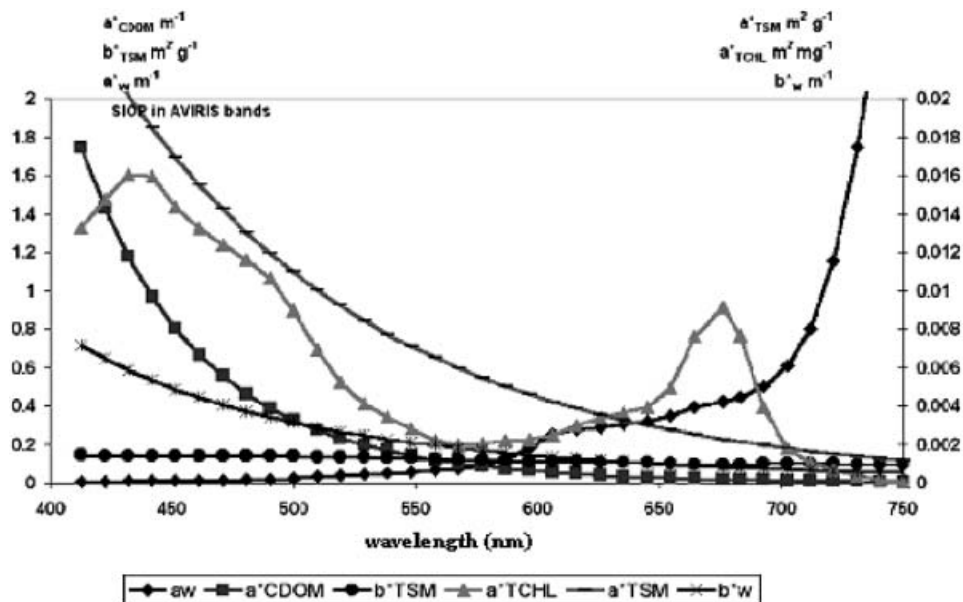

Figure 3. Measured SIOP were input into the forward Gordon's model to simulate spectra at St2 (Keyport Harbor) and St3 (Traid Bridge) locations for comparison with AVIRIS spectra.

of this inversion of the bio-optical model is obtained by substituting equation (1) into equation (2) and taking the correlation between TSM and CHL into account (Hoogenboom *et al.* 1998). Accordingly, the total TSM ($TSM_{tot} = TSM_{ph} + TSM_{ss}$) values include the part of the dry weight determined by the biomass of phytoplankton which is correlated to CHL concentration. The correlation coefficient can vary between 0.02 and 0.1 for freshwater algae (Gons *et al.* 1992). An average value of 0.07 ($TSM_{ph} = 0.07$ CHL) was used here based on Buiteveld (1990):

$$\left[a^*_{ph} + 0.07 a^*_{TSM} + 0.07 b^*_{bTSM} X \right] CHL + \left[a^*_{TSM} + b^*_{bTSM} X \right] TSM_{ss}$$
$$= -a_w - a^*_{CDOM} CDOM_{440} - b_{bw} X \tag{4}$$

where:

$$X = 1 - \frac{f}{R(0-)}$$

$$TSM_{ss} = TSM_{tot} - TSM_{ph} = TSM_{tot} - 0.07 CHL$$

Evaluating equation (3) for every wavelength of interest yields a set of equations, put into a matrix equation:

$$Y = \begin{pmatrix} A_{11} A_{12} \\ A_{21} A_{22} \end{pmatrix} \begin{pmatrix} CHL \\ TSM_{ss} \end{pmatrix} \tag{5}$$

where:

$$A_{m1} = a^*_{ph}(\lambda_m) + 0.07 a^*_{TSM}(\lambda_m) + 0.07 b^*_{bTSM}(\lambda_m) \left(1 - \frac{f}{R(\lambda_m)} \right)$$

$$A_{m2} = a^*_{TSM}(\lambda_m) + b^*_{bTSM}(\lambda_m) \left(1 - \frac{f}{R(\lambda_m)} \right)$$

$$y_m = -a_w(\lambda_m) - a^*_{CDOM}(\lambda_m) CDOM_{440} - b_{TSM}(\lambda_m) \left(1 - \frac{f}{R(\lambda_m)} \right)$$

In this basic case of matrix inversion one can solve this system for two concentrations from two spectral bands. In that case a two-by-two matrix has to be inverted analytically yielding the following expressions for the concentrations:

$$CHL = \frac{A_{22} y_1 - A_{12} y_2}{A_{11} A_{22} - A_{12} A_{21}} \text{ and } TSM_{ss} = \frac{-A_{21} y_1 + A_{11} y_2}{A_{11} A_{22} - A_{12} A_{21}} \tag{6}$$

3.4 *R(0-) calculation from AVIRIS calibrated radiance (at sensor observations)*

The AVIRIS sensor images the Earth's surface in 224 spectral bands approximately 10 nm wide covering the region 400–2500 nm from a NASA ER-2 aircraft at an altitude of 20 km. The ground resolution is 20 m × 20 m. The AVIRIS sensor records the integrated effects of the solar source, the atmosphere and the targeted surface. A major challenge is that approximately 90% of the signal received by the AVIRIS sensors originates in the atmosphere. Thus, removal of the atmospheric contribution to the measured radiance is a non-trivial problem. This requires careful consideration and assessment of:

1. The strength of the 760 nm oxygen absorption band measured in the AVIRIS spectrum through characterization of surface pressure height (Green 1991, Green *et al*. 1991, Green and Gao 1993);
2. The effect of aerosol scattering in the 400–700 nm region with an increasing effect toward shorter wavelengths (Green and Gao 1996); and
3. The influence of water vapour on the AVIRIS upwelling spectral radiance.

Due to these factors, a quantitative treatment of radiative transfer and atmospheric correction is the only way to achieve accurate (multi/hyperspectral) water leaving radiance measurements from satellite and airborne observations and to obtain accurate estimates of concentrations of optical water constituents.

To compensate for the atmospheric effects, first an atmospheric and air–water interface correction algorithm based on MODTRAN-4 was utilized. MODTRAN is a radiative transfer model developed by US Air Force Geophysical Laboratory which describes the radiative transfer process in the entire system from the solar source to the remote sensor via the hydrosols (Berk *et al*. 1989). The MODTRAN model simulates the radiance observed by a given senor–pixel–Sun geometry at a given altitude for a given surface albedo. One of the major characteristics of MODTRAN-4 is that the program allows a limited choice in controlling factors (such as atmosphere type and aerosol type) which makes it very attractive to the uneducated user but which also seriously limits the applicability. Of course, accurate measurements of the atmospheric composition can be entered into the program, but these measurements are generally not available during remote sensing overpasses, and the user interface for this type of control actions is rather complicated. In general, for water quality studies the standard parameters are adjusted until a match is found at some location between the remotely observed spectrum and the known spectrum at this location. There are two options: either the known spectrum is measured *in situ* during the overpass or the spectrum is modelled using known SIOP and measured concentrations during the overpass. In our case we found the following set of optimal input atmospheric parameters used in MODTRAN-4:

Horizontal visibility=20 km	Mid latitude summer atmosphere
urban (5 km) aerosol model	
Solar zenith angle=55°	Solar azimuth angle=83°
MODTRAN 16 streams mode	O_3 scaling factor=2.0

The above parameters were applied to the AVIRIS spectra where *in situ* measurements were collected during the course of the project (1999–2001). Results are shown in figure 4 indicating that MODTRAN-4 was able to bring the envelope of AVIRIS spectra reasonably close to simulated spectra. The above spectrum illustrates also that there are serious deviations from the expected shape of the spectrum. The following conclusions can be derived from this comparison and found to be consistent over the entire image:

1. There is considerable amount of spectral noise;
2. There are significant deviations in bands 675 and 702 nm (required for CHL mapping); and
3. There are unexplained large differences in the blue and near-infrared part of the spectrum.

Note that explanations for these errors are difficult to find. Experience from similar applications indicates that the MODTRAN standard range of coefficient
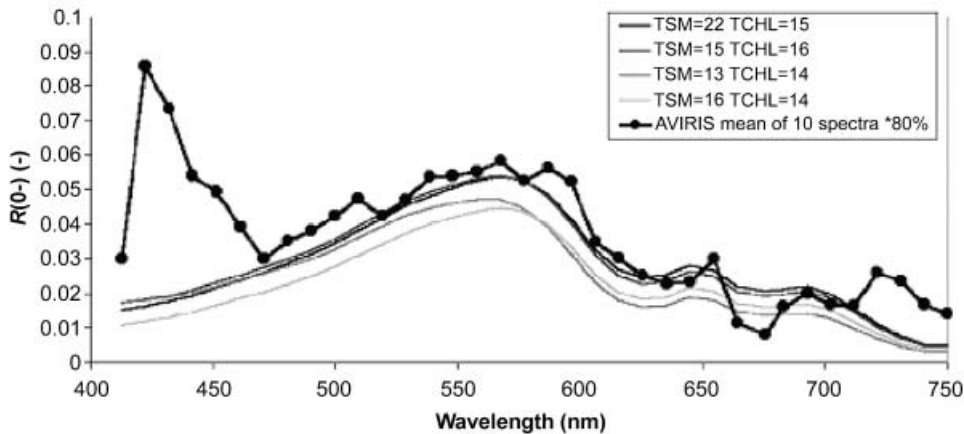
Figure 4. The simulated spectra using measured SIOP at St2 (Keyport Harbor) and St3 (Traid Bridge) locations compared with AVIRIS spectra.

settings basically allows a reasonable but never perfect retrieval of the water leaving reflectance spectrum. Image analysis indicates a considerable amount of sunglint present in the image which contributes to the spectral distortions. In addition, the standard AVIRIS calibration table used in calculation has not been verified for its accuracy.

4. Discussion and conclusion

In our approach IOP of water constituents were used to model the reflectance. A reasonable fit was found between modelled R(0-) using the optical model and atmospherically corrected AVIRIS data based on the MODTRAN-4 radiative transfer code. The result of the analysis as shown in figure 4 can be summarized as follows.

1. The spectra below 500 nm are uncorrectable and unreliable.
2. The envelope of the spectra is quite irregular, indicating that a substantial amount of sunglint within the AVIRIS data remains.
3. The irregularity of the spectra is such that the balance between 670 and 700 nm observations seems to be affected, making CHL determinations based on this ratio difficult.
4. The general shape of the envelope and the range of values seem to be realistic for 500 and 750 nm, although normally the spectral maximum is observed around 550 nm, but in this case it is skewed to the right.

(Note: The scaling difference may be due to many reasons; primarily to the time difference between the measurements.)

In view of these errors, an alternative approach was sought. In an attempt to avoid all possible calibration errors it was decided to correct the image for atmospheric influences using directly the simulated reflectance at a location where the concentrations are known and they vary little over time. The procedure used was simple and effective and involved the recalculation of the spectral bands in such a way that the pixel at the known location relatively matched the modelled spectrum.
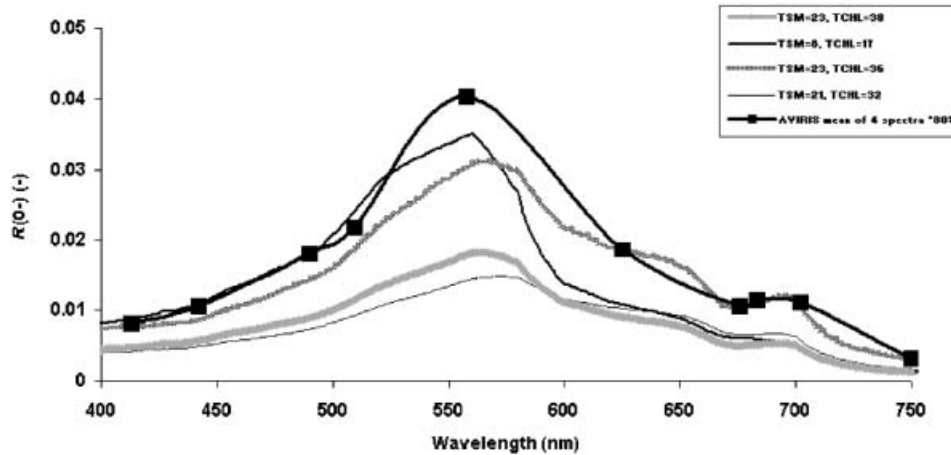
Figure 5. The atmospherically corrected AVIRIS spectrum (scaled down 20%) for comparison with simulated $R(0\text{-})$ representing different range of CHL and TSM concentrations.

Since validation of the atmospheric correction is very difficult due to a lack of simultaneous observations, the way to proceed is to calculate the concentrations of optically active constituents from the corrected image and to study the range and spatial distribution patterns of such concentrations. In this case, Peters (2001) hybrid iterative method was used to derive simultaneously the concentrations of CHL and TSM. Figure 5 shows that the spectra behave as expected for this water type at various stations within the study site.

Table 2 lists the measured and modelled concentration values as computed by the matrix inversion for the field sample locations marked on figure 1. There is a reasonable match between the calculated and measured concentrations for the WQP selected. The distributions of spatial patterns of CHL and TSM in the form of thematic maps are presented in figure 6.

In conclusion the AVIRIS spectral data provide the opportunity to distinguish the atmospheric effect from the marine water effect to set the estimated turbidity for retrieval of CHL concentration. An experiment with the Peters (2001) algorithm shows that simultaneous retrieval of TCHL, TSM and CDOM is possible based on AVIRIS observed spectra. Based on the results it was concluded that CHL and TSM show reasonable ranges and meaningful patterns. CDOM seems to be coupled to

Table 2. Retrieval of CHL and TSM concentrations from the AVIRIS atmospherically corrected data based on MODTRAN-4 using matrix inversion model (MIM) model (Hoogenboom *et al.* 1998).

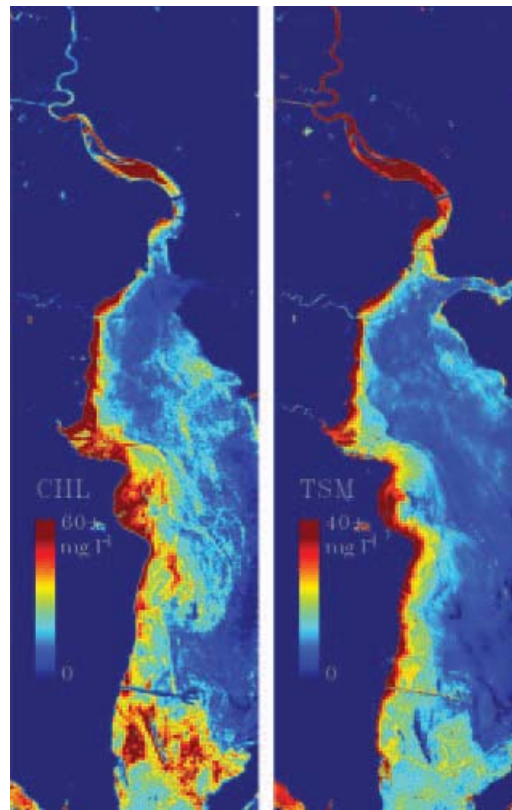| St	Location	Measured TCHL $(\mathrm{mg\,m^{-3}})$	Modelled TCHL ($\#2$) $(\mathrm{mg\,m^{-3}})$	Measured TSM $(\mathrm{g\,m^{-3}})$	Modelled TSM ($\#2$) $(\mathrm{g\,m^{-3}})$
3	Traid Bridge	17	9	13	19
4	Crookes Pt Staten Island	37	44	16	8
5	Comptons/PewsCreek	15	7	6	22
6	Keyport Harbor	32	12	26	19

Figure 6. AVIRIS image maps depicting the spatial distribution patterns of CHL and TSM for AVIRIS transect acquired over the study area on 13 July 2001.

CHL, which may be true in reality but which may also point to separation problems between these parameters because of insufficient resolution by the AVIRIS sensor, or because of incompleteness in the bio-optical model used.

Future research should focus on the development of a model for the coupled atmosphere–marine water which provides the link between the spectra measured by the AVIRIS spectrometers and the *in situ* measurements of spectral irradiances in the water. Overall, this work provides a reference baseline of remote sensing and *in situ* measurements that will have significance for future work on underwater light field and remote sensing methodology development for the Hudson/Raritan Estuary. Currently there is no systematic management tool for operational monitoring and prediction of pollution that is applicable to the Hudson/Raritan Estuary. Remote sensing can provide greater economy in such application than using conventional methods. The establishment of the IOP of the estuary and the *in situ* validation of bio-optical variables is a critical factor to use remote sensing as an operational monitoring/management tool. The output of remote sensing data analysis in forms of thematic maps (figure 6) representing the spatial distributions of WQP (i.e. CHL) can be integrated into a GIS. Such maps are important because of limited capability to monitor water quality conditions in the estuary using conventional methods.

Acknowledgments

References

BAGHERI, S. and DEKKER, A.G., 1999, Nearshore water quality assessment using bio-optical modeling and retrieval techniques. *Proceedings of the 8th JPL AVIRS Workshop, 8–12 February 1999* (Pasadena, CA: JPL).

BAGHERI, S., RIJKEBOER, M., PASTERKAMP, R. and DEKKER, A.G., 2000, Comparison of the field spectroradiometers in preparation for optical modeling. *Proceedings of the 9th JPL AVIRS Workshop* (Pasadena, CA: JPL), pp. 45–53.

BAGHERI, S., STAMNES, K. and LI, W., 2001, Application of radiative transfer theory to atmospheric correction of AVIRIS data. *Proceedings of the 10th JPL AVIRS Workshop* (Pasadena, CA: JPL), pp. 35–40.

BAGHERI, S., REIJKOBER, M. and GONS, H., 2002, Inherent and apparent optical measurements in the Hudson/Raritan Estuary. *Aquatic Ecology*, **36**, pp. 559–562.

BAGHERI, S., ZEHIN, C. and DIOS, R., 1999, Estimation of optical properties of nearshore water. *International Journal of Remote Sensing*, **20**, pp. 3393–3397.

BERK, A., BERSTIEN, L.S. and ROBERTSON, D.C., 1989, MODTRAN: a moderate resolution model for LOWTRAN7. Report GL-TR-89-0122, US Air Force Geophysical Laboratory, Hanscom, MA.

BUITEVELD, H., 1990, Uitzicht, a model for calculating secchi depth and extinction. Report 90.058, Rijkswarestaat, RIZA (in Dutch).

BUKATA, R.P., JEROME, J.H., KONRATYEV, K. and POZDNYAKOV, D.V., 1995, *Optical Properties and Remote Sensing of Inland and Coastal Waters* (Boca Raton: CRC Press).

DEKKER, A.G. and DONZE, M., 1994, In *Imaging Spectrometry as a Research Tool for Inland Water Resources Analysis*, edited by J. Hill (Dordrecht, The Netherlands: Kluwer AP), pp. 1–15.

DEKKER, A.G., HOOGENBOOM, H.J., GODDIJN, L.M. and MALTHUS, T.J.M., 1997, The relationship between inherent optical properties and reflectance spectra in turbid inland waters. *Remote Sensing Reviews*, **15**, pp. 59–74.

GONS, H.J., 1999, Optical teledetection of chlorophyll a in turbid inland waters. *Environmental Science and Technology*, **33**, pp. 1127–1132.

GONS, H.J., BURGER-WIERSMA, T., OTTEN, J.H. and RIJKEBOER, M., 1992, Coupling of phytoplankton and detritus in a shallow eutrophic lake (Lake Loosdrecht, The Netherlands). *Hydrobiologia*, **233**, pp. 51–59.

GONS, H., REIJKOBER, M., BAGHERI, S. and RUDDICK, K., 2000, Teledetection of chlorophyll-a in estuarine and coastal waters. *Environmental Science and Technology*, **34**, pp. 5189–5192.

GORDON, H.R., BROWN, O.B. and JACOBS, M.M., 1975, Computed relationships between inherent and apparent optical properties of a flat homogeneous ocean. *Applied Optics*, **14**, pp. 417–427.

GREEN, R.O., 1991, Retrieval of reflectance from AVIRIS-measured radiance using a radiative transfer code. *Proceedings of the 3rd JPL AVIRS Workshop*, JPL Publication 91-28 (Pasadena, CA: JPL), pp. 200–210.

GREEN, R.O., 1996, Summaries of the 6th JPL AVIRS Workshop. JPL, Pasadena, CA.

GREEN, R.O. and GAO, B.C., 1993, A proposed update to the solar irradiance spectrum used in LOWTRAN and MODTRAN. *Proceedings of the 4th JPL AVIRS Workshop*, JPL Publication 93-26 (Pasadena, CA: JPL), pp. 23–26.

GREEN, R.O., CONEL, J.E., MARGOLIS, J.S., BRUEGGE, C.J. and HOOVER, G.L., 1991, An inversion algorithm for retrieval of atmospheric and leaf water absorption from

AVIRIS radiance with compensation for atmospheric scattering. *Proceedings of the 3rd JPL AVIRS Workshop*, JPL Publication 91-28 (Pasadena, CA: JPL), pp. 51–61.

HAKVOORT, H., DE HAAN, H., JORDANS, R.W.L., VOS, R.J., PETERS, S.W.M. and RIJKEBOER, M., 2000, Towards operational airborne remote sensing of water quality in the Netherlands: validation and error analysis. Second EARSEL Workshop on Imaging Spectroscopy.

HOGE, F.E. and LYON, P.E., 1996, Satellite retrieval of inherent optical properties by linear matrix inversion of oceanic radiance models: an analysis of model and radiance measurement errors. *Journal of Geophysical Research*, **101**, pp. 16 631–16 648.

HOOGENBOOM, H.J., DEKKER, A.G. and DE HAAN, J.F., 1998, Retrieval of chlorophyll and suspended matter from imaging spectrometry data by matrix inversion. *Canadian Journal of Remote Sensing*, **24**, pp. 144–152.

JEFFRIES, H.P., 1962, Environmental characteristics of Raritan Bay, a polluted estuary. *Limnological Oceanography*, **7**, pp. 21–31.

KIRK, J.T.O., 1991, Volume scattering function, average cosines, and the underwater light field. *Limnological Oceanography*, **36**, pp. 455–467.

KIRK, J.T.O., 1994, *Light and Photosynthesis in Aquatic Ecosystems* (Cambridge, UK: University Press).

MOREL, A. and PRIEUR, L., 1977, Analysis of variations in ocean color. *Limnological Oceanography*, **22**, pp. 709–722.

NEN 6484, 1982, Water: determination of the content of not dissolved material and its ignition residue. Nederlands Normalisatie instituut, Delft, The Netherlands (in Dutch).

NEN 6520, 1981, Water: spectrophotometric determination of chlorophyll a content. Nederlands Normalisatie instituut, Delft, The Netherlands (in Dutch).

OEY, L.Y., MELLOR, G.L. and HIRES, R.I., 1985, A three-dimensional simulation of the Hudson/Raritan Estuary. Part I and II. *Journal of Geophysical Oceanography*, **15**, pp. 1676–1709.

PETERS, S.W.M., 2001, Analytical inversion methods for water quality parameter determination from remotely observed spectra. Report, Vrije Universiteit, The Netherlands.

RIJKEBOER, M., DEKKER, A.G. and HOOGENBOOM, H.J., 1998, Reflectance spectra with associated water quality parameters measured in Dutch waters (Speclib-TK-database). Institute for Environmental Studies, E98/12, The Netherlands.

VOS, R.J., DEKKER, A.G., PETERS, S.W.M., ROSSUM, G.V. and HOOIJKAAS, L.C., 1998, RESTWAQ2, part II. Comparison of remote sensing data, model results and in-situ data for the Southern Frisian Lakes. Report number NRSP-2 98-08b, Netherlands Remote Sensing Board (BCRS), Programme Bureau, Rijkswaterstaat Survey Department.

WHITLOCK, C.H., POOLE, L.R., USRY, J.W., HOUGHTON, W.M. and WITTE, W.G., 1981, Comparison of reflectance with backscatter and absorption parameters for turbid waters. *Applied Optics*, **20**, pp. 517–522.